

Transport properties and induced voltage in the structure of water-filled single-walled boron-nitrogen nanotubes

Quanzi Yuan and Ya-Pu Zhao^{a)}

State Key Laboratory of Nonlinear Mechanics (LNM), Institute of Mechanics, Chinese Academy of Sciences, Beijing 100190, People's Republic of China

(Received 13 February 2009; accepted 27 May 2009; published online 18 June 2009)

Density functional theory/molecular dynamics simulations were employed to give insights into the mechanism of voltage generation based on a water-filled single-walled boron-nitrogen nanotube (SWBNNT). Our calculations showed that (1) the transport properties of confined water in a SWBNNT are different from those of bulk water in view of configuration, the diffusion coefficient, the dipole orientation, and the density distribution, and (2) a voltage difference of several millivolts would generate between the two ends of a SWBNNT due to interactions between the water dipole chains and charge carriers in the tube. Therefore, this structure of a water-filled SWBNNT can be a promising candidate for a synthetic nanoscale power cell as well as a practical nanopower harvesting device. © 2009 American Institute of Physics. [DOI: [10.1063/1.3158618](https://doi.org/10.1063/1.3158618)]

I. INTRODUCTION

Water-filled nanotube structures have attracted considerable attention recently for their possible applications in the field of biological/chemical systems, electronic power converters, energy harvesting devices, etc.¹⁻³ The transport properties of water inside a nanotube are quite different from those of bulk water⁴⁻⁶ because the diameter of a nanotube is comparable to the size of confined water molecules. Král and Shapiro⁷ first theoretically predicted that electric current can be generated in metallic carbon nanotubes immersed in flowing liquid flowing along them. They believed that a phonon wind, which drags free carriers in the tube, is excited when liquid slips along the surface of a nanotube. Then Ghosh *et al.*^{8,9} found that a voltage of several millivolts was generated in the carbon nanotube along the flowing direction and proposed an explanation based on pulsating asymmetric ratchets. Zhao *et al.*¹⁰ designed elegant experiments and realized power converters based on de-ionized water-filled single-walled carbon nanotubes (SWCNTs). Due to the interactions between water dipoles and electron carriers in nanotubes, the electric current in a tube can drive water transportation as a motor, and the water flow in a tube can induce voltage between the two ends of the tube as a generator. Recently, Yuan and Zhao¹¹ simulated the voltage induced by the structure of water-filled SWCNT by using the mutual iterative methods of density functional theory (DFT) and molecular dynamics (MD). But there is no theoretical or experimental work available about the structure of water-filled single-walled boron-nitrogen nanotubes (SWBNNTs). Because of the excellent physical and chemical properties, the regular atomic structures of a SWBNNT,¹²⁻¹⁵ as well as a stronger interaction with the single-file water chain in a SWBNNT, we believe that the structure of water-filled SWBNNTs might also be developed as nanovoltage generators or energy harvesting devices. In this work we give insights into (1) the transport properties of water in the tube from the aspects of configuration, the diffusion coefficient, the dipole orientation, and the density distribution, and (2) the mechanism of voltage generation

^{a)} Author to whom correspondence should be addressed. Electronic mail: yzhao@imech.ac.cn.

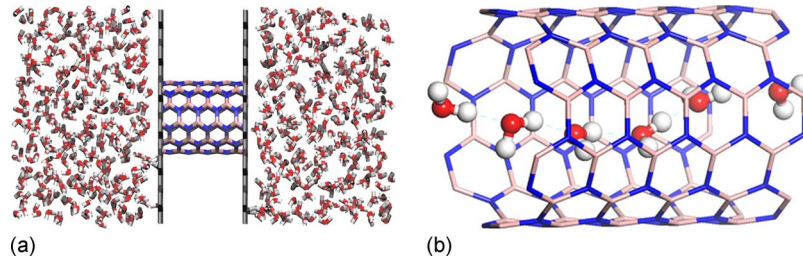


FIG. 1. (a) Visualization of the MD simulation domain. (b) Visualization of the DFT simulation domain. Blue, pink, red, and white atoms represent nitrogen, boron, oxygen, and hydrogen atoms, respectively. The light blue dashed lines between water molecules represent hydrogen bonds. The curve of the single-file water chain presents a helicoidal configuration.

using the mutual iterative methods of DFT and MD. We predict that SWBNNT will be a promising candidate for a synthetic nanoscale power cell and support the development of practical nanopower harvesting devices.

II. METHODOLOGY

We first performed MD simulations on an uncapped finite-length armchair-type (6, 6) SWBNNT, which was 12.56 Å in length and 8.31 Å in diameter, to obtain the filling structure. The MD calculation domain consisted of a BN nanotube, water molecules, and two layers of graphene with a hole in them to avoid interaction with water molecules near the two ends of the nanotube. The nanotube and graphene layers were fixed, as shown in Fig. 1(a). The boron and nitrogen atoms of BNNT were modeled as charged Lennard-Jones (LJ) particles initially. The charges on B and N atoms are 0.39 and $-0.39e$ according to Won and Aluru's work,¹⁵ respectively. The LJ parameters for a SWBNNT were $\sigma_{B-B}=0.3453$ nm, $\epsilon_{B-B}=0.0950$ kJ/mol, $\sigma_{N-N}=0.3365$ nm, and $\epsilon_{N-N}=0.1450$ kJ/mol according to the COMPASS force field.¹⁶ The TIP4P water model¹⁷ was used to simulate the behaviors of water molecules. The water monomers are represented by four interaction sites, three on the nuclei and one on a point M located on the HOH bisector of 0.125 Å from oxygen toward the hydrogen atoms. There are charges of $0.5242e$ on the hydrogen atoms and $-1.0484e$ on M . The LJ parameters for water molecules are $\sigma_{O-O}=0.316435$ nm, $\epsilon_{O-O}=0.68355$ kJ/mol, $\sigma_{H-H}=0$ nm, and $\epsilon_{H-H}=0$ kJ/mol.

In the experiments, a typical method for studying water channels is to set up different concentrations of solutes on the two sides of the channel, giving rise to an osmotic pressure difference. Thus, water flux and velocity could be measured.^{8,18,19} The experimental condition was simulated by applying a constant force on a layer of bulk water molecules. Consequently a pressure gradient was induced between the two ends of a SWBNNT. Following the method proposed by Zhu *et al.*²⁰ and examined by Wan *et al.*²¹ and Li *et al.*,²² an external force along the nanotube $+z$ axial direction was applied to the O atoms of water molecules whose coordinates (in the unit cell of the periodic system) satisfy $0 < z < 8$ Å in our simulation. The corresponding pressure is 150 MPa. The values of σ and ϵ between them were calculated according to the Lorentz-Berthelot rule: $\sigma_{x-y}=(\sigma_{x-x}+\sigma_{y-y})/2$ and $\epsilon_{x-y}=(\epsilon_{x-x}\times\epsilon_{y-y})^{1/2}$. The particle-particle particle-mesh method²³ with a 10^{-4} precision was used for each time step to compute long-range Coulombic interactions. The equations of motion were integrated by using the leapfrog algorithm.

The simulations were performed for 5 ns with a 1.0 fs time step under a constant temperature of 300 K using LAMMPS.²⁴ The characteristic time for dipolar reorientation in an uncharged tube is in approximate nanoseconds, while that for a single water molecule in bulk fluid is in approximate picoseconds. Therefore the simulations can fully reflect all the behaviors of the filling structure without losing any motion of the water molecules. The water molecules in the tube were pushed by the hydrogen bonds between the water molecules and formed a dipole chain along the z direction, as illustrated in Fig. 1(b).

Then we studied the influence of a dipole chain on the electronic performance of a nanotube. To investigate the effect of water molecules on the charge distribution of a tube, we used

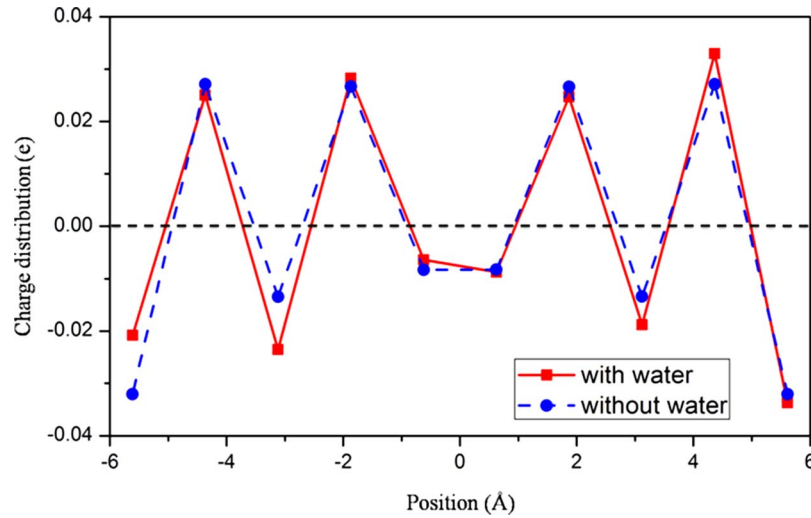


FIG. 2. Charge distribution on atoms of a (6, 6) SWBNNT without water molecules (blue dashed line) and with water molecules (solid red line) calculated using DFT. The charges were averaged for the atoms with the same axial position.

GAUSSIAN 03 (Ref. 25) to calculate the four different transient configurations obtained from MD simulations, which consisted of a SWBNNT and the water molecules inside the tube and near the tube entrance. The Becke, three-parameter, Lee–Yang–Parr (B3LYP) method with 6-31g** basis was used to fully consider the interactions between the water dipoles and charge carriers in the tube. To explore the dipole moment in this system, convergence criteria for the self-convergence field were set to be “tight.” The charges from electrostatic potentials using a grid based method (CHELPG) scheme was used to calculate partial charges on atoms, as not to vary widely with theoretical method and basis set.

Then, parameters calculated by DFT simulations were substituted back into MD simulations to obtain transport properties. In this way, interactions between water molecules and tube were taken into account.

III. RESULTS AND DISCUSSIONS

The CHELPG charge distribution on the atoms in the (6, 6) BNNT without and with the confined water molecules is illustrated in Fig. 2. The charges are averaged for the atoms with the same axial position in view of symmetry.

The transport properties of confined water in tube were calculated based on the CHELPG charge distribution and found to be different from that of bulk water. In the present work, we first evaluated the transport properties by computing the self-diffusion coefficient. Since water molecules form a single-file chain in a (6, 6) BNNT, we consider only water diffusion in the axial direction of a BNNT. The axial diffusion coefficient D_z of water is related to the slope of the water mean-squared displacement (MSD) by the Einstein relation

$$D_z = \frac{1}{2} \lim_{t \rightarrow \infty} \frac{\langle |\vec{r}(t) - \vec{r}(0)|^2 \rangle}{\Delta t}, \quad (1)$$

where $\vec{r}(t) - \vec{r}(0)$ is the distance traveled by molecule i over some time interval of length Δt , and the squared magnitude of this vector is averaged (as indicated by the angle brackets) over many such time intervals. The diffusion coefficient of water inside a BNNT is $(1.55 \pm 0.05) \times 10^{-5} \text{ cm}^2/\text{s}$, which is significantly less than that of the bulk water of $2.69 \times 10^{-5} \text{ cm}^2/\text{s}$.²⁶ The confined water molecules are bounded by the size of the tube wall. On the basis of MSD analysis, the confined water molecules in the tube were found to be solidlike, indicating a hampered atomic mobility.

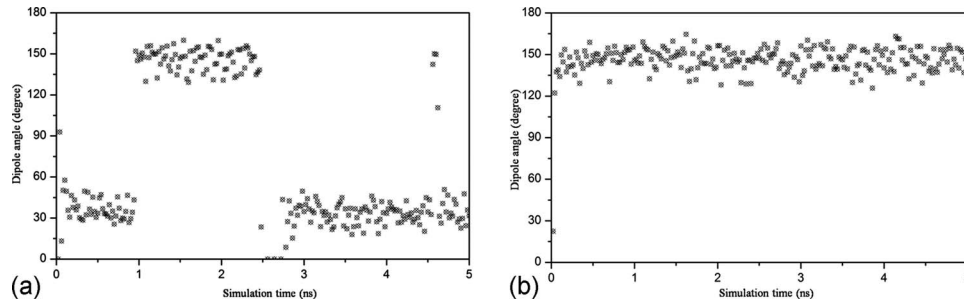


FIG. 3. Dipole angles of water molecules with respect to simulation time (a) in a BNNT with initial charge and (b) in a BNNT with differential charge. Each point is the average of water dipoles per frame. The water dipole orientation angle is defined as the angle between the water dipole vector and the tube axis z . 0° denotes the water dipole vector pointing along the $+z$ direction.

As shown in Fig. 2, we can find that the charge distribution is symmetric when no water molecule enters. When water is conducted, the symmetry is broken by oriented water dipoles. The atoms of the BNNT act as acceptors, receiving the charges from the water molecules, and make the total charges of the tube negative. The charge distribution becomes asymmetric. In this way, the single-file water chain results in the polarity of a SWBNNT. The total charges on the left are $0.0305e$ and on the right are $-0.0437e$. A finite element electrostatic model is used to calculate the electric potential in the calculation domain,

$$U_k = \sum_i \frac{Q_i}{4\pi\epsilon_0 r_{ik}}, \quad (2)$$

where U_k is the electric potential at position k , ϵ_0 is the vacuum permittivity where $\epsilon_0 = 8.854 \times 10^{-12}$ F/m, Q_i represents the charge of atom i , and r_{ik} is the distance between atom i and position k . Then the voltage difference between the two ends of a BNNT can be obtained, $\Delta U = U_u - U_l = 14.9$ mV, which is at the same order of magnitude compared to the voltage measured in the experiment.^{8,10} The voltage between the two ends of tube induces an electric field $E = U/d \sim 10^7$ V/m. The highly oriented single-file water chain is responsible for the extremely high electric field in a BNNT. The inner diameter of the tube is 8.31 \AA , which is comparable to the size of a water molecule of about 2.5 \AA . So water molecules inside the (6, 6) BNNT can only move as a single file. First, water molecules form hydrogen bonds between them, hence to gain binding energy and to make the total free energy become minimum. So this water-filled SWCNT structure becomes more stable. Geometry optimization²⁷ and MD simulations²⁸ validate that this oriented water chain has the minimum energy. Second, the induced dipole on a BNNT has a reverse orientation with the water dipoles, which attract water single file to be oriented.

Two problems, i.e., the end effect of the BNNT and the flip of water dipoles, disturb the voltage generation in the process of water transportation in a SWBNNT. The end effect of the BNNT, which is visualized in Fig. 2, causes a phenomenon where charges at the end of the tube are much more than those in the middle of the tube. The water dipoles would be affected by this end effect, which makes the average water dipoles in the BNNT become zero, raises an L defect, and results in symmetric distribution of water dipoles in the tube. Using the charge distribution on the tube with water molecules and subtracting the charge distribution without water molecules, we can get the differential charge distribution. This differential charge distribution can approximately represent charge distribution on a long BNNT without being affected by the end effect. We compare the dipole angles of water molecules with respect to simulation time in the initial and later BNNT in Fig. 3. As shown in Fig. 3(a), the water dipoles flip about every 2 ns, resulting in a nearly zero dipole angle on average. Hence the induced voltage would not be stable. But once we placed the differential charge distribution in the MD simulation, we found the water dipoles pointed toward one end of the tube and did not flip in the simulated duration due to the effect of

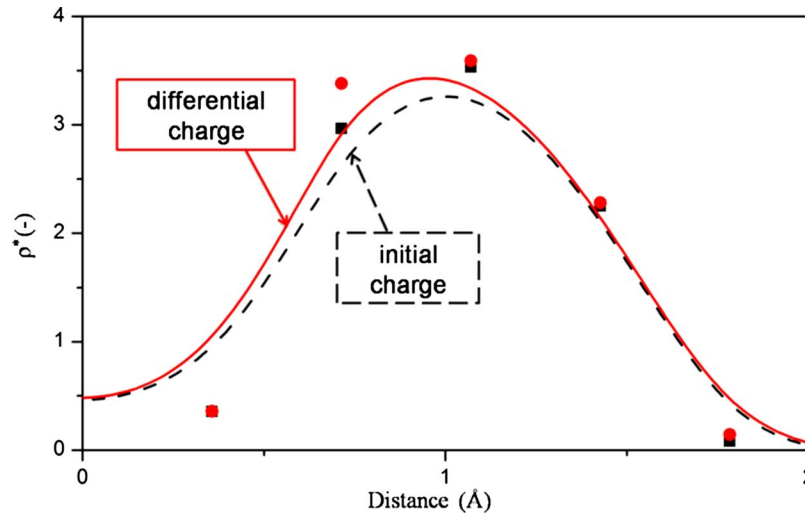


FIG. 4. Radial local water density distributions $\rho^* = \rho_c / \rho_b$ vs the distance from the axis of the tube in the tube with initial charge (black dashed line) and differential charge (solid red line), where ρ_c is the actual density in the tube and ρ_b is the density of bulk water.

the opposite dipoles on the tube wall induced by the water dipoles, as shown in Fig. 3(b). The average dipole angle is 146.5° , hence a stable voltage is induced. The water chain with an unchanged orientation produced a constant voltage difference between the two ends of the tube (note that the direction and voltage difference fluctuate slightly).

Radial local water density distributions in the tube with initial charge and differential charge are illustrated in Fig. 4. The radial local water density distribution is expressed by

$$\rho^* = \frac{\rho_c}{\rho_b}, \quad (3)$$

where ρ_c and ρ_b are the densities of confined water in tube and bulk water, respectively. First, we find that most water molecules prefer staying at the position of about 1 \AA away from the center of the tube. Taking into account the structure of a single-file water chain in the tube, as shown in Fig. 1(b), we find that the water chain is a helicoidal structure. Second, the water molecules prefer staying along the axis of the tube with a differential charge compared to those in the tube with initial charge.

IV. CONCLUSION

In summary, we have shown that (1) the transport properties of water in BNNT are different from those of bulk water. The diffusion coefficient of confined water is significantly less than that of bulk water. The single-file water chain keeps a stable dipole orientation. The water molecules in the tube distribute mainly 1 \AA away from the center of the tube, presenting a helicoidal structure. (2) A voltage can be generated by a water-filled SWBNNT. Our calculations showed that two effects, i.e., the end effect and the flip of water dipoles, influence the process of voltage generation. It is also demonstrated that interactions between the water dipole chains and charge carriers in a tube can result in charge redistribution in a SWBNNT with the DFT/MD method, causing a voltage difference of several millivolts between the two ends of the tube. Therefore, this structure of a water-filled SWBNNT may be a promising candidate for a synthetic nanoscale power cell as well as a practical nanopower harvesting device.

ACKNOWLEDGMENTS

This work was jointly supported by the National High-tech R&D Program of China (863 Program, Grant Nos. 2007AA04Z348 and 2007AA021803), National Basic Research Program of China (973 Program, Grant No. 2007CB310500), and National Natural Science Foundation of China (NSFC, Grant Nos. 10772180 and 10721202).

- ¹D. Mattia and Y. Gogotsi, *Microfluid. Nanofluid.* **5**, 289 (2008).
- ²A. Noy, H. G. Park, F. Fornasiero, J. K. Holt, C. P. Grigoropoulos, and O. Bakajin, *Nanotoday* **2**, 22 (2007).
- ³M. Whitby and N. Quirke, *Nat. Nanotechnol.* **2**, 87 (2007).
- ⁴G. Hummer, J. C. Rasaiah, and J. P. Noworyta, *Nature (London)* **414**, 188 (2001).
- ⁵Y. C. Liu and Q. Wang, *Phys. Rev. B* **72**, 085420 (2005).
- ⁶D. J. Mann and M. D. Halls, *Phys. Rev. Lett.* **90**, 195503 (2003).
- ⁷P. Král and M. Shapiro, *Phys. Rev. Lett.* **86**, 131 (2001).
- ⁸S. Ghosh, A. K. Sood, and N. Kumar, *Science* **299**, 1042 (2003).
- ⁹S. Ghosh, A. K. Sood, S. Ramaswamy, and N. Kumar, *Phys. Rev. B* **70**, 205423 (2004).
- ¹⁰Y. C. Zhao, L. Song, K. Deng, Z. Liu, Z. X. Zhang, Y. L. Yang, C. Wang, H. F. Yang, A. Z. Jin, Q. Luo, C. Z. Gu, S. S. Xie, and L. F. Sun, *Adv. Mater. (Weinheim, Ger.)* **20**, 1772 (2008).
- ¹¹Q. Z. Yuan and Y. P. Zhao, *J. Am. Chem. Soc.* **131**, 6374-6376 (2009).
- ¹²X. Blase, A. Rubio, S. G. Louie, and M. L. Cohen, *Europhys. Lett.* **28**, 335 (1994).
- ¹³Y. Chen, J. Zou, S. J. Campbell, and G. Le Caer, *Appl. Phys. Lett.* **84**, 2430 (2004).
- ¹⁴C. Y. Won and N. R. Aluru, *J. Am. Chem. Soc.* **129**, 2748 (2007).
- ¹⁵C. Y. Won and N. R. Aluru, *J. Phys. Chem. C* **112**, 1812 (2008).
- ¹⁶H. Sun, *J. Phys. Chem. B* **102**, 7338 (1998).
- ¹⁷W. L. Jorgensen, J. Chandrasekhar, J. D. Madura, R. W. Impey, and M. L. Klein, *J. Chem. Phys.* **79**, 926 (1983).
- ¹⁸M. Majumder, N. Chopra, R. Andrews, and B. J. Hinds, *Nature (London)* **438**, 44 (2005).
- ¹⁹A. Kalra, S. Garde, and G. Hummer, *Proc. Natl. Acad. Sci. U.S.A.* **100**, 10175 (2003).
- ²⁰F. Q. Zhu, E. Tajkhorshid, and K. Schulten, *Biophys. J.* **83**, 154 (2002).
- ²¹R. Z. Wan, J. Y. Li, H. J. Lu, and H. P. Fang, *J. Am. Chem. Soc.* **127**, 7166 (2005).
- ²²J. Y. Li, X. J. Gong, H. J. Lu, D. Li, H. P. Fang, and R. H. Zhou, *Proc. Natl. Acad. Sci. U.S.A.* **104**, 3687 (2007).
- ²³R. W. Hockney and J. W. Eastwood, *Computer Simulation Using Particles* (Hilger, London, 1989).
- ²⁴S. Plimpton, *J. Comput. Phys.* **117**, 1 (1995).
- ²⁵M. J. Frisch, G. W. Trudes, H. B. Schlegel *et al.*, GAUSSIAN03, Revision D.01, Gaussian, Inc., Wallingford, CT, 2004.
- ²⁶R. J. Mashl, S. Joseph, N. R. Aluru, and E. Jakobsson, *Nano Lett.* **3**, 589 (2003).
- ²⁷C. Y. Won, S. Joseph, and N. R. Aluru, *J. Chem. Phys.* **125**, 114701 (2006).
- ²⁸A. Waghe, J. C. Rasaiah, and G. Hummer, *J. Chem. Phys.* **117**, 10789 (2002).